doi:10.1016/S0022-2836(02)01177-4 *J. Mol. Biol.* (2003) **325**, 1–10

JMB

Available online at www.sciencedirect.com

SCIENCE DIRECT®

Nucleic Acid Conformational Changes Essential for HIV-1 Nucleocapsid Protein-mediated Inhibition of Self-priming in Minus-strand Transfer

Minh K. Hong[1], Elizabeth J. Harbron[2], Donald B. O'Connor[2] Jianhui Guo[3], Paul F. Barbara[2], Judith G. Levin[3] and Karin Musier-Forsyth[1]*

[1]*Department of Chemistry University of Minnesota 207 Pleasant Street S.E. Minneapolis, MN 55455-0431 USA*

[2]*Department of Chemistry and Biochemistry University of Texas Austin, TX 78712, USA*

[3]*NICHD, NIH, Bethesda MD 20892, USA*

**Corresponding author*

Reverse transcription of the HIV-1 genome is a complex multi-step process. HIV-1 nucleocapsid protein (NC) is a nucleic acid chaperone protein that has been shown to greatly facilitate the nucleic acid rearrangements that precede the minus-strand transfer step in reverse transcription. NC destabilizes the highly structured transactivation response region (TAR) present in the R region of the RNA genome, as well as a complementary hairpin structure ("TAR DNA") at the 3′-end of the newly synthesized minus-strand strong-stop DNA ((−) SSDNA). Melting of the latter structure inhibits a self-priming (SP) reaction that competes with the strand transfer reaction. In an *in vitro* minus-strand transfer system consisting of a (−) SSDNA mimic and a TAR-containing acceptor RNA molecule, we find that when both nucleic acids are present, NC facilitates formation of the transfer product and the SP reaction is greatly reduced. In contrast, in the absence of the acceptor RNA, NC has only a small inhibitory effect on the SP reaction. To further investigate NC-mediated inhibition of SP, we developed a FRET-based assay that allows us to directly monitor conformational changes in the TAR DNA structure upon NC binding. Although the majority (~71%) of the TAR DNA molecules assume a folded hairpin conformation in the absence of NC, two minor "semi-folded" and "unfolded" populations are also observed. Upon NC binding to the TAR DNA alone, we observe a modest shift in the population towards the less-folded states. In the presence of the RNA acceptor molecule, NC binding to TAR DNA results in a shift of the majority of molecules to the unfolded state. These measurements help to explain why acceptor RNA is required for significant inhibition of the SP reaction by NC, and support the hypothesis that NC-mediated annealing of nucleic acids is a concerted process wherein the unwinding step occurs in synchrony with hybridization.

Keywords: FRET; chaperone activity; nucleocapsid protein; self-priming; TAR

Introduction

Reverse transcription in retroviruses is a complex process that results in synthesis of a linear double-stranded DNA from the single-stranded genomic RNA template.[1] The HIV nucleocapsid protein (NC) stimulates this process, which involves a number of nucleic acid rearrangements, including tRNA primer annealing and two strand transfer events.[1–9] Thus, NC is a nucleic acid "chaperone" protein that facilitates nucleic acid

Abbreviations used: HIV-1, human immunodeficiency virus type 1; NC, nucleocapsid protein; FRET, fluorescence resonance energy transfer; SP, self-priming; (−) SSDNA, minus-strand strong-stop DNA; TAR, transactivation response region; TAR DNA, complementary sequence to TAR; Cy3, indocarbocyanine-3; FL, 6-carboxyfluorescein; nt, nucleotide(s); RT, reverse transcriptase.

E-mail address of the corresponding author: musier@chem.umn.edu

0022-2836/03/$ - see front matter

conformational changes to form the most thermodynamically stable interactions in an ATP-independent fashion.[10–14]

HIV-1 NC is a 55 amino acid, highly basic, nucleic acid-binding protein. The mature form, also known as NCp7, is generated by cleavage of the viral Gag precursor protein.[15–17] NC contains two CCHC metal-binding motifs, which form tandem zinc finger structures connected by a short linker sequence.[18,19] We have recently shown that the zinc finger structures are critical for NC's nucleic acid chaperone activity.[20–23] The CCHC zinc fingers are also required for full chaperone activity of FIV NCp8 *in vitro*.[24] In addition, NC's zinc fingers appear to impart preferential binding to single-stranded nucleic acids.[21,25–27]

Despite NC's apparent preference for binding single-stranded nucleic acids, the preference is modest,[28] consistent with its role in interacting with both single and double-stranded RNA and DNA molecules during reverse transcription. NC greatly facilitates tRNA primer annealing to the HIV genome. However, it has been shown that NC binding to tRNA alone does not induce global unwinding of the tRNA structure,[29,30] but rather causes more subtle changes in the tertiary and secondary structural motifs.[30,31] Thus, at least in the case of tRNA annealing, NC binding does not facilitate tRNA unwinding in the absence of the complementary primer binding site, i.e. unwinding occurs simultaneously with annealing.

Following tRNA primer annealing, minus-strand strong-stop DNA ((−) SSDNA) is synthesized and then translocated to the 3′ terminus of the viral RNA genome, in a reaction mediated by base pairing of the complementary repeat (R) regions in (−) SSDNA and viral RNA. NC has been shown to stimulate minus-strand transfer by increasing the rate of intermolecular annealing and by blocking a competing intramolecular self-priming (SP) reaction.[4,7,32,33] SP occurs due to the presence of a highly structured sequence at the 3′-end of the (−) SSDNA.[1,4,7,34] This sequence, which is complementary to the TAR element at the 5′-end of the genome, will hereafter be referred to as "TAR DNA". The TAR DNA sequence has the potential to fold back onto itself and form a hairpin, which can self-prime DNA synthesis and form a heterogeneous mixture of minus-strand DNA products with plus-strand extensions.[7]

The presence of HIV NC in *in vitro* minus-strand transfer assay systems has been shown to reduce the extent of TAR-dependent self-priming.[7,32,33,35] However, whether NC inhibition of SP is due to direct destabilization of the TAR DNA hairpin, or whether the reduction of SP in these *in vitro* systems is dependent on the presence of the TAR RNA acceptor strand is an open question. Lapadat-Tapolsky *et al*. originally reported that SP is inhibited by NC in the absence of an RNA acceptor.[32] More recently, Hughes and co-workers have shown that NC can significantly inhibit SP from a 100-nt synthetic (−) SSDNA oligonucleotide only in the presence of a 17-nt DNA oligomer complementary to the 3′-end of the (−) SSDNA.[33] The size of the DNA oligomer is similar to that of short RNA oligomers formed as a result of RNase H degradation of the RNA template during (−) SSDNA synthesis.[33,36]

Recently, using both absorbance and fluorescence spectroscopy, Mély and co-workers have directly examined NC's effect on the structure of a 55-nt TAR DNA hairpin mimic.[37] This work showed that binding of an NC-derived peptide containing the zinc finger motifs, (12-55)NCp7, enhances the intrinsic fraying of the ends of the TAR DNA hairpin, and results in melting of 7–8 bp. However, the effect of NC binding on the TAR DNA structure in the presence of acceptor RNA was not probed. Nevertheless, taken together with the data of Hughes and co-workers discussed above, these results imply that partial melting of the TAR DNA hairpin may not be sufficient to reduce SP, at least in the absence of a complementary nucleic acid.

To examine this hypothesis and to gain further insights into NC's role as a nucleic acid chaperone protein in the minus-strand transfer step of reverse transcription, we carried out both biochemical and FRET-based assays. Using a modified *in vitro* minus-strand transfer assay system,[7] we investigated NC's effect on the amount of SP products formed in the absence and presence of acceptor RNA. In addition, we used a FRET-based approach to directly monitor structural changes in the TAR DNA hairpin in the presence and absence of both NC and acceptor RNA. We found that NC binding to the TAR DNA hairpin alone causes partial unfolding of the hairpins. Under these conditions, very little NC-dependent inhibition of SP is observed. We also established that the acceptor RNA is required for significant inhibition of SP in this system. Moreover, in the presence of the acceptor RNA, the majority of the TAR DNA molecules are present in an unfolded state. Taken together, our data support the conclusion that the conformational changes observed upon NC binding to the TAR DNA alone are not sufficient to inhibit SP and promote strand transfer, and that substantial unwinding of the TAR DNA hairpin occurs only in the presence of the acceptor RNA.

Result

NC effects on TAR-dependent self-priming

Previously, we showed that NC has the ability to promote the annealing step in minus-strand transfer[20,22,38] and to reduce the formation of undesired SP products.[7] In these assays, the acceptor RNA was always present and the effect of NC on the SP reaction in the absence of the complementary RNA was not reported. To address this question, we assayed DNA synthesis in the absence and presence of acceptor RNA. As shown

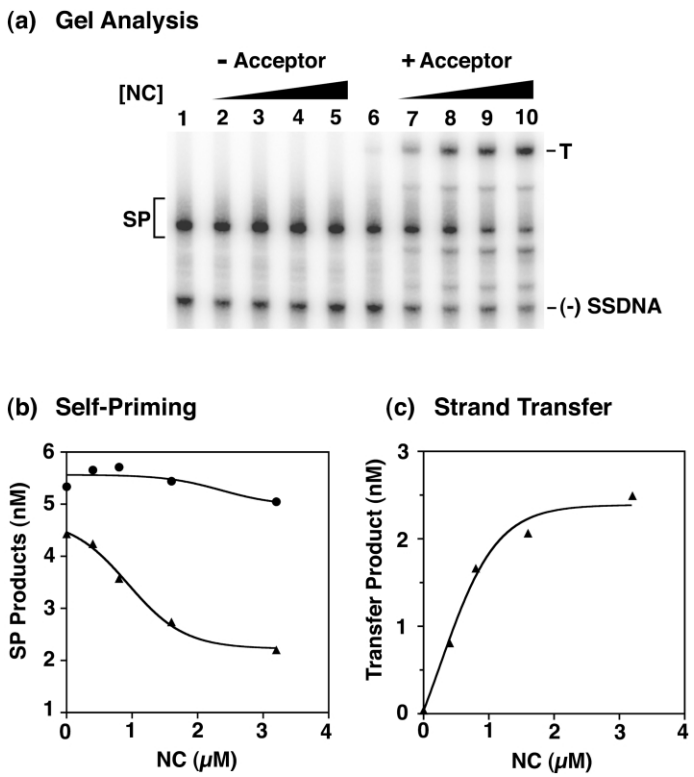

Figure 1. NC's effect on SP in the absence and presence of acceptor RNA. (a) Gel analysis showing the effect of NC and 148-nt acceptor RNA on SP. The major bands are indicated as follows: (−) SSDNA, the 128-nt DNA containing the complementary TAR element; SP, SP products; and T, the 182-nt strand transfer product. The minus NC controls are shown in lane 1, 10 nM TAR DNA alone, and lane 6, 10 nM TAR DNA plus 10 nM acceptor RNA. The effect of increasing amounts of NC on SP in the absence (lanes 2–5) and presence (lanes 7–10) of 148-nt acceptor RNA is also shown. The concentrations of NC are 0.4 μM (7 nt/NC) (lanes 2 and 7), 0.8 μM (3.5 nt/NC) (lanes 3 and 8), 1.6 μM (1.75 nt/NC) (lanes 4 and 9), and 3.2 μM (0.875 nt/NC) (lanes 5 and 10). (b) Graph quantifying NC's effect on the amount of SP products in the absence (closed circles) and presence (closed triangles) of acceptor RNA. (c) Graph quantifying the amount of strand transfer product as a function of increasing concentrations of NC. The graphs in panels (b) and (c) are based on the data shown in panel (a).

in Figure 1(a), in the absence of NC, the predominant band observed corresponds to the SP products, which form both in the absence or presence of acceptor RNA (lanes 1 and 6, respectively). With the addition of increasing amounts of NC to the reactions carried out in the absence of acceptor RNA (lanes 2–5), NC does not substantially inhibit the formation of the SP products. In contrast, in the presence of acceptor RNA, addition of increasing amounts of NC results in a corresponding increase in formation of the strand transfer product, with a concomitant decrease in SP products (Figure 1(a), lanes 7–10). Figures 1(b) and (c) graphically show these results. In particular, we find that NC inhibits the formation of SP products and stimulates formation of the transfer product in a dose-dependent manner, but only in the presence of the acceptor RNA.

FRET system used to probe NC-induced TAR DNA conformational changes

The inability of NC to significantly affect the formation of SP products in the absence of acceptor

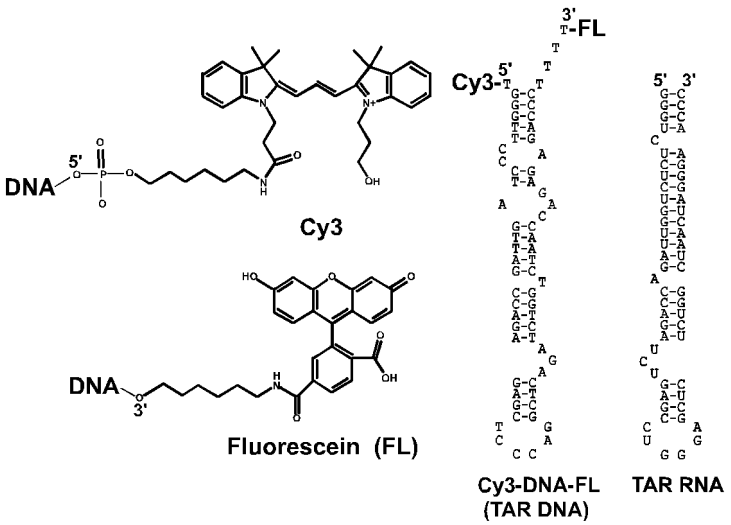

Figure 2. Structures of fluorophores and oligonucleotides used in the FRET assay. Indocarbocyanine-3 (Cy3) was used as the acceptor dye molecule and was attached to the 5′-dT of the DNA *via* a succinimidyl ester (C_6–NH) linker. 6-Carboxyfluorescein (FL) was used as the donor dye molecule and was attached to the 3′-dT of the DNA *via* a succinimidyl ester (C_6–NH) linker. Also depicted are predicted secondary structures for the TAR DNA (64 nt) and TAR RNA (59 nt) used in the FRET studies.

RNA suggests that under these conditions NC is unable to melt the TAR DNA secondary structure. However, a recent study probing NC's effect on a TAR DNA mimic that is similar, although not identical to the TAR DNA used in the present study, concluded that (12–55)NCp7 does induce partial melting and fraying of the ends of the hairpin.[37] To directly investigate this possibility in our system, a fluorescence resonance energy transfer (FRET) assay was developed in which fluorescent donor and acceptor molecules were covalently attached to a DNA oligonucleotide mimicking the TAR DNA hairpin at the 3′-end of (−) SSDNA (Figure 2). Using the energy transfer properties of fluorescent molecules that are in close proximity, FRET can be used as a "molecular ruler" to measure conformational changes of oligonucleotides in solution.[39,40] In our system, the 64-nt TAR DNA mimic was labeled on the 5′ and 3′-ends with acceptor (indocarbocyanine-3 (Cy3)) and donor (6-carboxyfluorescein (FL)) dyes, respectively. This construct retained the sequence of the core TAR hairpin (59 nt), but to facilitate chemical synthesis and to prevent any undesired G residue quenching effects,[41,42] a 5′-T and 3′-TTTT overhang were added to the sequence. The 3′ overhang also prevents formation of a dark non-fluorescent state that can form due to close proximity of the two dyes.[37] Similarly, a truncated 59-nt version of the TAR RNA hairpin was used as the acceptor RNA in our FRET system (Figure 2). All FRET measurements were carried out using the fully mature 55-amino acid HIV-1 NC protein.[43]

Characterization of dye-labeled DNA

Singly-labeled Cy3–DNA and DNA–FL, as well as doubly-labeled Cy3–DNA–FL were gel-purified and were each determined to be >95% free from other contaminants by electrospray ionization mass spectrometry. The Förster radius, R_O, was calculated to be 63 Å (see Materials and Methods). Figure 3(a) shows the normalized fluorescence emission spectra for the singly-labeled DNA–FL (orange), as well as for the doubly-labeled Cy3–DNA–FL (red). FL emission in the doubly-labeled sample is substantially quenched relative to its emission in DNA–FL, indicative of efficient energy transfer to Cy3. A concomitant increase in Cy3 emission at 570 nm is also observed. Addition of TAR RNA to Cy3–DNA–FL in the absence of NC does not alter the emission spectrum (data not shown), indicating that the mutual presence of the TAR RNA and the TAR DNA is insufficient for annealing. Upon addition of NC in the absence of acceptor RNA, an increase in FL emission and concomitant decrease in Cy3 emission are observed (Figure 3(a), purple). In the presence of both acceptor TAR RNA and NC, an even larger change in the emission intensities of Cy3–DNA–FL is observed (Figure 3(a), green), suggesting further NC-induced conformational changes under these conditions. These spectral

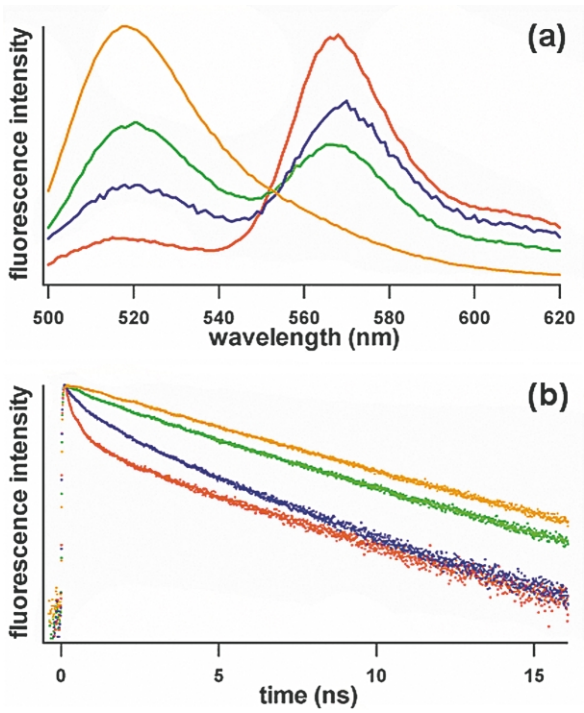

Figure 3. FRET spectra showing NC's effect on the singly and doubly-labeled TAR DNA in the absence and presence of TAR RNA. (a) Steady-state fluorescence spectra of 75 nM DNA–FL (orange), Cy3–DNA–FL (red), Cy3–DNA–FL with NC (4 nt/NC, purple), and Cy3–DNA–FL and 112.5 nM TAR RNA with NC (4 nt/NC, green) under conditions outlined in Materials and Methods. All spectra were normalized by integrating the area between 500 nm and 630 nm. (b) Time-resolved fluorescence spectra. Shown is the semi-logarithmic plot of the fluorescence decays of the samples described in (a).

changes correspond to conformational changes that cannot be quantitatively evaluated by steady-state FRET, but that are further characterized by time-resolved FRET measurements as described below.

Time-resolved FRET measurements were carried out to more quantitatively describe the NC-induced conformational changes of the TAR DNA observed in the steady-state experiments. Fluorescence lifetimes of the labeled TAR DNA constructs in the presence and absence of TAR RNA and NC were measured by time-correlated single photon counting (TCSPC). Figure 3(b) shows the decay of DNA–FL emission (orange), which is well described by a single exponential with a fluorescence lifetime (τ_1) of 4.0 ns (Table 1). The emission of Cy3–DNA–FL (red) is significantly quenched relative to DNA–FL due to FRET from the donor FL to the acceptor Cy3 dye. The decay of Cy3–DNA–FL is best described by a triple exponential, indicating the presence of at least three DNA conformations with different donor–acceptor dye distances. The three populations are designated the "hairpin", "semi-folded", and

Table 1. Time-resolved fluorescence data and analysis

Sample	τ_1, ns[a] (%)	τ_2, ns (%)	τ_3, ns (%)	R, Å[b]
Before NC addition				
DNA–FL	4.0 ± 0.01 (100)	–	–	–
Cy3–DNA–FL	3.6 ± 0.08 (10)	0.6 ± 0.2 (19)	0.1 ± 0.06 (71)	34
DNA–FL/RNA	4.0 ± 0.01 (100)	–	–	–
Cy3–DNA–FL/RNA	3.6 ± 0.03 (10)	0.5 ± 0.09 (21)	0.1 ± 0.02 (69)	34
After NC addition				
DNA–FL	4.1 ± 0.02 (86)	0.6 ± 0.09 (14)	–	–
Cy3–DNA–FL	3.3 ± 0.1 (22)	1.2 ± 0.1 (34)	0.2 ± 0.03 (44)	37
DNA–FL/RNA	4.0 ± 0.02 (81)	0.4 ± 0.08 (19)	–	–
Cy3–DNA–FL/RNA	4.0 ± 0.1 (53)	1.6 ± 0.4 (22)	0.2 ± 0.07 (25)	>100

[a] Lifetime values are an average of at least five measurements. The average amplitude (percent of total signal) for each component is given in parentheses. In the case of DNA–FL, τ_1 represents the major component, whereas τ_2 represents a minor component observed following the addition of NC. In the case of Cy3–DNA–FL, the three lifetimes represent hairpin (τ_3), semi-folded (τ_2), and unfolded (τ_1) populations, as discussed in the text.
[b] FRET distance for the major component only. See Materials and Methods for calculation parameters.

"unfolded" states based on the FRET distances calculated from their fluorescence lifetimes. Approximately 71% of the Cy3–DNA–FL population is in the hairpin state, which is characterized by a lifetime (τ_3) of 0.1 ns and a corresponding FRET distance (R) of 34 Å (Table 1). The unfolded state ($\tau_1 = 3.6$ ns, $R = 90$ Å) shows very little FRET quenching, while the semi-folded population ($\tau_2 = 0.6$ ns, $R = 46$ Å) represents an intermediate case. As expected from the steady-state FRET data, addition of TAR RNA to either DNA–FL or Cy3–DNA–FL did not significantly alter the DNA conformations (Table 1).

Using the FRET behavior of Cy3–DNA–FL as a baseline, conformational changes and/or population shifts in TAR DNA upon addition of NC and the acceptor RNA were next quantitatively evaluated. The addition of NC to Cy3–DNA–FL yields a minor reduction in FRET quenching (Figure 3(b), purple). Although this decay fits to a triple exponential with similar lifetimes as measured for Cy3–DNA–FL alone (red), the population in the presence of NC is shifted toward the less-folded conformations. The unfolded population (τ_1) increases from 10% to 22% in the presence of NC relative to Cy3–DNA–FL alone, whereas the semi-folded population (τ_2) increases from 19% to 34% (Table 1). By contrast, a much more significant decrease in FRET quenching is observed when both TAR RNA and NC are added to Cy3–DNA–FL (Figure 3(b), green). This decrease is consistent with NC-mediated TAR DNA:TAR RNA annealing, which would be expected to induce a substantial population shift from the hairpin state to the unfolded conformation. A triple exponential decay was again fit to the emission decay. The largest population of molecules (53%) now corresponds to the longest lived component (τ_1), with a lifetime of 4.0 ns. The latter corresponds to a FRET distance of >100 Å (Table 1), consistent with an annealed complex. Moreover, the observed increase in the unfolded state population is in good agreement with the percent annealing observed *via* gel-shift analysis (see below).

Gel-shift annealing assays

In order to visualize the extent of annealing by an independent method, gel-shift annealing assays were performed under assay conditions that were identical to those used in the FRET measurements (see Material and Methods). When ^{32}P-labeled TAR DNA alone was run on a native gel, multiple broad bands were observed, indicating that the TAR DNA in solution was conformationally heterogeneous (Figure 4, lane 1). Consistent with this hypothesis a DNA *m*Fold[44] analysis predicted that the TAR DNA could fold into multiple structures with similar energies at 25 °C (40 mM NaCl, 1 mM $MgCl_2$; data not shown). This observation is also in good agreement with the time-resolved FRET analysis, which indicated the presence of at least three populations

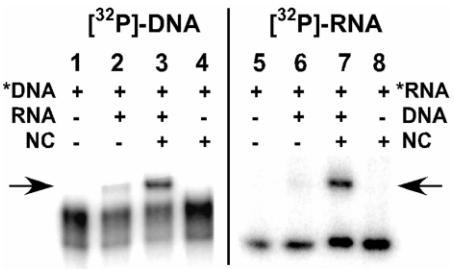

Figure 4. Gel-shift annealing assays using FRET conditions. Non-denaturing 15% polyacrylamide gel showing NC-mediated annealing of the TAR DNA:TAR RNA oligonucleotides. Lanes 1–4: 75 nM [^{32}P]-labeled TAR DNA (indicated by an asterisk) in the absence or presence of 112.5 nM TAR RNA and NC (4 nt/NC), as indicated above the lanes. Lanes 5–6: 75 nM [^{32}P]-labeled TAR RNA (indicated by an asterisk) in the absence or presence of 112.5 nM TAR DNA and NC (4 nt/NC). Arrows indicate the migration of the binary complex.

of molecules for the Cy3–DNA–FL construct (Table 1).

Also in accord with FRET results and with earlier reports on annealing in minus-strand transfer,[4,20,38,45] addition of the RNA acceptor to the TAR DNA does not produce substantial (<5%) binary complex formation after a 40 minute incubation in the absence of NC (Figure 4, lane 2). Even a prolonged six-hour incubation of the nucleic acids does not result in a substantial increase in uncatalyzed binary complex formation (data not shown). However, substantial binary complex (30–40%) is observed in the presence of both RNA and NC (Figure 4, lane 3), with the extent of the reaction reaching a plateau after approximately 30 minutes (data not shown). The percent of annealed complex observed in the gel-shift assays is in general agreement with the amount of binary complex formation observed based on the FRET analysis. Due to the stability of the individual TAR hairpin elements, annealing does not go to completion under the conditions of the FRET assays. By increasing the concentration of the oligonucleotides, complete NC-induced annealing could be achieved (data not shown). In contrast, in the absence of RNA, TAR DNA with NC does not result in any noticeable band shift, confirming that DNA:DNA duplex formation does not occur (Figure 4, lane 4). The annealing reactions were repeated using ^{32}P-labeled TAR RNA with similar results (Figure 4, lanes 5–8). As expected, the TAR RNA alone migrates as a single species on the non-denaturing gel (lane 5). Once again, substantial (~40%) complex formation occurs in the presence of both NC and TAR DNA (lane 7). To confirm that the probes did not interfere with the extent of NC-mediated annealing, annealing assays were also performed with the dye-labeled Cy3–DNA–FL and ^{32}P-labeled TAR RNA. The extent of annealing was similar to that observed for the unlabeled DNA, confirming that the probes do not significantly inhibit binary complex formation (data not shown).

Discussion

In the present work, we have used both biochemical and FRET-based assays to investigate NC's activity in a system that models minus-strand transfer, an essential step in reverse transcription of the HIV-1 retroviral genome. We demonstrate that both NC and the acceptor RNA must be present in order to facilitate strand transfer and to inhibit a competing SP reaction, i.e. NC alone is insufficient to block SP of the TAR hairpin in (−) SSDNA (Figure 1). These results are in general agreement with those of Hughes and co-workers, who demonstrated that, in the absence of acceptor RNA, NC inhibits formation of SP products from (−) SSDNA, only in the presence of complementary DNA oligomers designed to mimic RNase H degradation products.[33,36]

To gain further insights into the effects of NC binding on the structure of the (−) SSDNA hairpin both in the absence and presence of acceptor RNA, we used a FRET-based approach. Using truncated versions of (−) SSDNA (TAR DNA, 64 nt) and acceptor RNA (59 nt), we find that NC binding to the DNA alone results in a shift in the population distribution of TAR DNA molecules towards the unfolded and semi-folded states (Table 1). Thus, NC binding decreases the stability of the TAR DNA, in good agreement with previous studies using a truncated version of NC, (12–55)NCp7, and an alternate TAR DNA mimic.[37] This conclusion is also consistent with results of Summers and co-workers who have observed by NMR that NC binding increases the "conformational lability" of an 18-nt (−) PBS DNA mimic.[46] The NC-induced conformational changes of TAR DNA observed in the absence of acceptor RNA are more substantial than changes observed upon NC binding to the tRNA^{Lys,3} primer.[29–31] As shown by native gel electrophoresis, *m*FOLD analysis, and FRET, the TAR DNA hairpin is conformationally heterogeneous and predicted to be inherently much less stable than tRNA. Thus, NC's ability to induce nucleic acid conformational changes in the absence of a complementary sequence will vary depending on the stability of the starting structure.

A model to explain NC-facilitated strand transfer *versus* formation of SP products that is consistent with the data presented here is shown in Figure 5. Although NC binding to TAR DNA

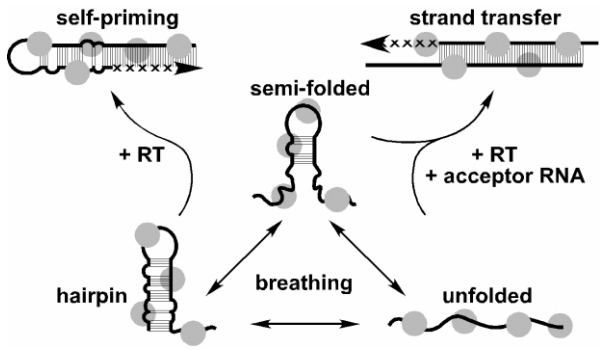

Figure 5. Model for NC's effect on SP in the absence and presence of acceptor RNA. In the absence of acceptor RNA, NC (represented as a gray ball) binds to the (−) SSDNA (hairpin, semi-folded, and unfolded populations), increasing the thermal fluctuations (breathing) of the nucleic acids. An equilibrium state is achieved with the majority of the (−) SSDNA in the hairpin conformation from which RT can initiate formation of the SP products. NC may then redistribute the less-folded populations towards the more folded hairpin structure, which in turn produces more SP products. In the presence of the acceptor RNA, NC-induced breathing of the (−) SSDNA results in complete unwinding and annealing of the two complementary hairpin sequences, allowing RT to form the desired strand transfer product. NC is also likely to induce breathing of the TAR RNA hairpin (not shown), but this was not investigated in the present work.

alone destabilizes the population of molecules and likely induces "breathing", which allows the DNA hairpins to sample alternate conformations more readily, the folded hairpin conformation is still the most dominant conformation observed in our FRET analysis. In the presence of reverse transcriptase (RT), SP products can form as a result of priming from the hairpin species. Although we have arbitrarily assigned the three observed lifetimes to three distinct populations of Cy3–DNA–FL, the distribution is likely to be dynamic. Thus, as the hairpin species are removed from the population of molecules due to self-priming, NC may facilitate conversion of the semi-folded species to hairpins from which self-priming can now be initiated. Therefore, this breathing model helps to explain why the addition of NC alone to the TAR DNA does not significantly decrease SP products formation (Figure 1). Our FRET-based measurements show that much more substantial unfolding of the TAR DNA occurs in the presence of NC and the acceptor RNA (Figure 5). Under these conditions, formation of SP products is also reduced and transfer product is formed (Figure 1). Thus, significant NC-induced unwinding of the TAR DNA hairpin and subsequent reduction in SP occurs in synchrony with the annealing step of strand transfer.

These results provide further support for a general model for NC's nucleic acid chaperone activity.[21] In particular, NC binding to both RNA and DNA induces subtle conformational changes, including partial structural destabilization and increased breathing of double-stranded helical regions. Although the increased conformational flexibility induced by NC binding is not generally sufficient to globally unwind or linearize nucleic acids, it allows them to sample alternate conformational states more readily such that in the presence of a complementary oligonucleotide the most thermodynamically stable intermolecular duplex can readily form.

Material and Methods

Protein purification

All of the proteins used in this work were obtained or prepared according to previously published procedures as follows: HIV-1 RT,[7] wild-type NC,[43] and T7 RNA polymerase.[47]

Nucleic acid preparation

Singly-labeled DNA oligonucleotides containing either 5′-Cy3 or 3′-FL (Cy3–DNA and DNA–FL, respectively), as well as the doubly-labeled DNA (Cy3–DNA–FL), were obtained from TriLink Biotechnologies (San Diego, CA). The oligonucleotides were purified on 12% denaturing polyacrylamide gels and determined to be greater than 95% pure by electrospray ionization mass spectrometry performed in the lab of Dr Natalia Tretyakova (University of Minnesota). The unlabeled 64-nt DNA oligonucleotide was obtained from the MicroChemical Facility (University of Minnesota), subjected to denaturing polyacrylamide gel purification, and stored in diethyl pyrocarbonate-treated water at −20 °C. For gel-shift annealing assays, the chemically synthesized TAR DNA was 5′-radiolabeled with [γ-^{32}P]-ATP and T4 polynucleotide kinase (New England Biolabs, Beverly, MA). The truncated 59-nt TAR RNA was prepared *via in vitro* transcription using a PCR-amplified template encoding the 59-nt sequence downstream of a T7 RNA polymerase promoter. Internally [^{32}P]-labeled RNA was transcribed *in vitro* under similar conditions, except that the GTP concentration was lowered from 4 mM to 1 mM and the reaction was supplemented with 17 mCi/ml [α-^{32}P]-GTP. The synthetic 128-nt (−) SSDNA used in the strand transfer assays was obtained from IDT (Coralville, IA) and was labeled at its 5′-end with ^{32}P.[48] The 148-nt acceptor RNA was prepared from *Fsp* I-linearized plasmid pJA by *in vitro* transcription with T7 RNA polymerase, as described.[7]

Minus-strand transfer assays

Assays were performed using a 128-nt ^{32}P-labeled synthetic (−) SSDNA (1×10^6–2×10^6 cpm) and a 148-nt acceptor RNA, as described.[7] Briefly, (−) SSDNA (final concentration, 10 nM) was added to reaction buffer (50 mM Tris–HCl, pH 8.0; 75 mM KCl; and 1 mM dithiothreitol); this was followed by addition of acceptor RNA (final concentration, 10 nM), as specified in the figure legend, and increasing amounts of HIV-1 NC. HIV-1 RT (0.2 pmol) was then added and DNA synthesis was initiated by adding $MgCl_2$ (final concentration, 7 mM) and the four deoxynucleoside triphosphates (each at a final concentration of 100 μM). Following incubation at 37 °C for 30 minutes, reactions were terminated by the addition of EDTA (final concentration, 50 mM), followed by proteinase K treatment and phenol:chloroform extraction (1:1). Reactions were loaded onto a 6% sequencing gel; the labeled DNA products were visualized and quantified using a PhosphorImager (Molecular Dynamics) and ImageQuant software.

Gel-shift annealing assays

Prior to use, all oligonucleotides were refolded at a concentration of 1 μM in 25 mM Hepes, pH 7.5 and 40 mM NaCl, by incubation at 80 °C (two minutes) and 60 °C (two minutes), followed by addition of $MgCl_2$ to a final concentration of 10 mM and placement on ice. [^{32}P]-labeled TAR DNA or RNA (75 nM) were combined with a 1.5-fold excess of complementary RNA or DNA, respectively, in a solution containing 25 mM Hepes, pH 7.5 and 40 mM NaCl. HIV-1 NC was added at a ratio of 4 nt/NC and samples were incubated at room temperature. After 40 minutes, the reactions were quenched by proteinase K (Sigma) treatment, extracted twice with phenol:chloroform, and the products separated by SDS-15% polyacrylamide gel electrophoresis (acrylamide to bisacrylamide, 19:1, w/w). The bands were visualized using a Bio-Rad Molecular Imager FX and quantified with Bio-Rad Quantity One software.

Steady-state FRET experiments

Steady-state fluorescence spectra (corrected) were recorded at room temperature by exciting the samples at 490 nm using a PTI spectrofluorimeter (model QM-2000; Photon Technology International, Lawrenceville,

NJ). Emission was collected through a Glan-Thompson prism set at the "magic angle". The fluorescence measurements were performed under the identical conditions (excluding the proteinase K treatment and phenol:chloroform extractions) as the gel-shift annealing assays. NC induces a blue shift in FL emission and affects the emission intensity, as previously reported.[37] Therefore, in order to evaluate the effect of NC on TAR DNA conformation, spectra of Cy3–DNA–FL were corrected for this phenomenon.

Time-resolved FRET experiments

Time-resolved fluorescence data were measured by time-correlated single photon counting at 22 °C with 488 nm vertically polarized excitation pulses ($\Delta t \sim 200$ fs, repetition rate of 3.8 MHz) from a mode-locked Ti:sapphire laser system (Coherent Mira 900, Coherent pulse picker model 9200, Inrad SHG/THG model 5-050). Emission was detected at 90° with respect to the excitation axis with a microchannel plate detector (Hamamatsu R3809U-50) through a 520 nm bandpass filter (20 nm FWHM) and a Glan–Taylor polarizer (Karl Lambrecht) set at the magic angle. The time-resolved anisotropy was calculated from emission decays measured with the polarizer alternately in a vertical or horizontal position.[49] All emission decays were fit using an iterative nonlinear least squares fitting procedure in which decay data was fit to a sum of exponential decays convoluted with the instrument response function (FWHM ~ 50 ps).

Determination of the Förster radius

The Förster radius (R_O), the distance at which the energy transfer rate is equal to the decay rate, was determined to be 63 Å according to:

$$R_O = [8.7585 \times 10^{-5}(\kappa^2 \Phi_D J/\eta^4)]^{1/6} \quad (1)$$

where κ is the orientation factor, Φ_D is the donor quantum yield in the absence of the acceptor, η is the refractive index of the medium, and J is the spectral overlap integral. The quantum yield of the donor in the absence of the acceptor was determined to be 0.38 based on a known standard of fluorescein at pH 13 (quantum yield = 0.92 ± 0.03[50]). The value of η used was 1.33 based on the refractive index of water at 22 °C. A value of 2/3 was assumed for κ^2 based on time-resolved and steady-state anisotropy measurements. Steady-state methods were used to determine a value of 0.28 for the anisotropy of the Cy3 acceptor dye. The initial anisotropy, $r(0)$, of FL donor emission in both Cy3–DNA–FL and Cy3–DNA–FL heat annealed to RNA acceptor was 0.3, which decayed to ~0 in less than 1.1 ns. This result implies that the FL donor undergoes uninhibited rotational freedom and justifies the use of $\kappa^2 = 2/3$.[49,51] The spectral overlap integral, J, was calculated to be 8.96×10^{15} M^{-1} cm^{-1} nm^4 by numerical integration of the emission spectrum of DNA–FL and the absorption spectrum of Cy3–DNA.

FRET distance calculations

The FRET efficiency (ε) was calculated from steady-state data according to:

$$\varepsilon = 1 - (I_{DA}/I_D) \quad (2)$$

where I_{DA} and I_D are the peak fluorescence intensity of FL in Cy3–DNA–FL and DNA–FL, respectively. The efficiency of energy transfer is related to the distance between the two probe molecules (R) according to Förster theory:[52]

$$\varepsilon = [1 + (R/R_O)^6]^{-1} \quad (3)$$

where R_O is the Förster radius, which is given in equation (1) above. R was calculated from time-resolved data according to:

$$R = \frac{R_O}{\left(\frac{\tau_D}{\tau_{DA}} - 1\right)^{1/6}} \quad (4)$$

where τ_{DA} and τ_D are the lifetimes of donor FL in Cy3–DNA–FL and DNA–FL, respectively, and R_O is again the Förster radius.

Acknowledgements

We thank Drs Natalia Tretyakova and Soobong Park for carrying out the mass spectrometry of the dye-labeled DNA oligonucleotides. We also thank Dr Wai-Tak Yip for assistance with data analysis as well as helpful discussion, and Dr Susan Heilman-Miller for valuable discussion and critical reading of the manuscript. We are grateful to Dr. Robert Gorelick for supplying some of the pure recombinant NC protein used in this work. This research was supported by NIH grant AI65056 (K.M.-F), NIH postdoctoral NRSA grant F32 AI10463 (E.J.H.), and NIH predoctoral training grant T32 GM08277 (M.K.H.).

References

1. Coffin, J. M., Hughes, S. H. & Varmus, H. E. (1997). *Retroviruses*, Cold Spring Harbor Laboratory Press, Plainview, NY.
2. De Rocquigny, H., Gabus, C., Vincent, A., Fournié-Zaluski, M. C., Roques, B. & Darlix, J. L. (1992). Viral RNA annealing activities of human immunodeficiency virus type 1 nucleocapsid protein require only peptide domains outside the zinc fingers. *Proc. Natl Acad. Sci. USA*, **89**, 6472–6476.
3. Allain, B., Lapadat-Tapolsky, M., Berlioz, C. & Darlix, J. L. (1994). Transactivation of the minus-strand DNA transfer by nucleocapsid protein during reverse transcription of the retroviral genome. *EMBO J.* **13**, 973–981.
4. You, J. C. & McHenry, C. S. (1994). Human immunodeficiency virus nucleocapsid protein accelerates strand transfer of the terminally redundant sequences involved in reverse transcription. *J. Biol. Chem.* **269**, 31491–31495.
5. DeStefano, J. J. (1995). Human immunodeficiency virus nucleocapsid protein stimulates strand transfer from internal regions of heteropolymeric RNA templates. *Arch. Virol.* **140**, 1775–1789.
6. Rodríguez-Rodríguez, L., Tsuchihashi, Z., Fuentes, G. M., Bambara, R. A. & Fay, P. J. (1995). Influence of human immunodeficiency virus nucleocapsid protein on synthesis and strand transfer by the reverse transcriptase *in vitro*. *J. Biol. Chem.* **270**, 15005–15011.

7. Guo, J., Henderson, L. E., Bess, J., Kane, B. & Levin, J. G. (1997). Human immunodeficiency virus type 1 nucleocapsid protein promotes efficient strand transfer and specific viral DNA synthesis by inhibiting TAR-dependent self-priming from minus-strand strong-stop DNA. *J. Virol.* **71**, 5178–5188.
8. Auxilien, S., Keith, G., Le Grice, S. F. & Darlix, J. L. (1999). Role of post-transcriptional modifications of primer $tRNA^{Lys,3}$ in the fidelity and efficacy of plus strand DNA transfer during HIV-1 reverse transcription. *J. Biol. Chem.* **274**, 4412–4420.
9. Wu, T., Guo, J., Bess, J., Henderson, L. E. & Levin, J. G. (1999). Molecular requirements for human immunodeficiency virus type 1 plus-strand transfer: analysis in reconstituted and endogenous reverse transcription systems. *J. Virol.* **73**, 4794–4805.
10. Tsuchihashi, Z. & Brown, P. O. (1994). DNA strand exchange and selective DNA annealing promoted by the human immunodeficiency virus type 1 nucleocapsid protein. *J. Virol.* **68**, 5863–5870.
11. Darlix, J. L., Lapadat-Tapolsky, M., de Rocquigny, H. & Roques, B. P. (1995). First glimpses at structure-function relationships of the nucleocapsid protein of retroviruses. *J. Mol. Biol.* **254**, 523–537.
12. Herschlag, D. (1995). RNA chaperones and the RNA folding problem. *J. Biol. Chem.* **270**, 20871–20874.
13. Rein, A., Henderson, L. E. & Levin, J. G. (1998). Nucleic-acid-chaperone activity of retroviral nucleocapsid proteins: significance for viral replication. *Trends Biochem. Sci.* **23**, 297–301.
14. Lorsch, J. R. (2002). RNA chaperones exist and DEAD Box proteins get a life. *Cell*, **109**, 797–800.
15. Mervis, R. J., Ahmad, N., Lillehoj, E. P., Raum, M. G., Salazar, F. H., Chan, H. W. & Venkatesan, S. (1988). The gag gene products of human immunodeficiency virus type 1: alignment within the gag open reading frame, identification of posttranslational modifications, and evidence for alternative gag precursors. *J. Virol.* **62**, 3993–4002.
16. Henderson, L. E., Bowers, M. A., Sowder, R. C., II, Serabyn, S. A., Johnson, D. G., Bess, J. W., Jr *et al.* (1992). Gag proteins of the highly replicative MN strain of human immunodeficiency virus type 1: posttranslational modifications, proteolytic processings, and complete amino acid sequences. *J. Virol.* **66**, 1856–1865.
17. Swanstrom, R. & Wills, J. W. (1997). Synthesis, assembly, and processing of viral proteins. In *Retroviruses* (Coffin, J. M., Hughes, S. H. & Varmus, H. E., eds), pp. 263–334, Cold Spring Harbor Laboratory Press, Plainview, NY.
18. South, T. L., Kim, B., Hare, D. R. & Summers, M. F. (1990). Zinc fingers and molecular recognition. Structure and nucleic acid binding studies of an HIV zinc finger-like domain. *Biochem. Pharmacol.* **40**, 123–129.
19. Summers, M. F., Henderson, L. E., Chance, M. R., Bess, J. W., Jr, South, T. L., Blake, P. R. *et al.* (1992). Nucleocapsid zinc fingers detected in retroviruses: EXAFS studies of intact viruses and the solution-state structure of the nucleocapsid protein from HIV-1. *Protein Sci.* **1**, 563–574.
20. Guo, J., Wu, T., Anderson, J., Kane, B. F., Johnson, D. G., Gorelick, R. J. *et al.* (2000). Zinc finger structures in the human immunodeficiency virus type 1 nucleocapsid protein facilitate efficient minus- and plus-strand transfer. *J. Virol.* **74**, 8980–8988.
21. Williams, M. C., Rouzina, I., Wenner, J. R., Gorelick, R. J., Musier-Forsyth, K. & Bloomfield, V. A. (2001). Mechanism for nucleic acid chaperone activity of HIV-1 nucleocapsid protein revealed by single molecule stretching. *Proc. Natl Acad. Sci. USA*, **98**, 6121–6126.
22. Guo, J., Wu, T., Kane, B. F., Johnson, D. G., Henderson, L. E., Gorelick, R. J. & Levin, J. G. (2002). Subtle alterations of the native zinc finger structures have dramatic effects on the nucleic acid chaperone activity of human immunodeficiency virus type 1 nucleocapsid protein. *J. Virol.* **76**, 4370–4378.
23. Williams, M. C., Gorelick, R. J. & Musier-Forsyth, K. (2002). Specific zinc-finger architecture required for HIV-1 nucleocapsid protein's nucleic acid chaperone function. *Proc. Natl Acad. Sci. USA*, **99**, 8614–8619.
24. Moscardini, M., Pistello, M., Bendinelli, M., Ficheux, D., Miller, J. T., Gabus, C. *et al.* (2002). Functional interactions of nucleocapsid protein of feline immunodeficiency virus and cellular prion protein with the viral RNA. *J. Mol. Biol.* **318**, 149–159.
25. Priel, E., Aflalo, E., Seri, I., Henderson, L. E., Arthur, L. O., Aboud, M. *et al.* (1995). DNA binding properties of the zinc-bound and zinc-free HIV nucleocapsid protein: supercoiled DNA unwinding and DNA-protein cleavable complex formation. *FEBS Letters*, **362**, 59–64.
26. Berglund, J. A., Charpentier, B. & Rosbash, M. (1997). A high affinity binding site for the HIV-1 nucleocapsid protein. *Nucl. Acids Res.* **25**, 1042–1049.
27. Fisher, R. J., Rein, A., Fivash, M., Urbaneja, M. A., Casas-Finet, J. R., Medaglia, M. & Henderson, L. E. (1998). Sequence-specific binding of human immunodeficiency virus type 1 nucleocapsid protein to short oligonucleotides. *J. Virol.* **72**, 1902–1909.
28. Urbaneja, M. A., Wu, M., Casas-Finet, J. R. & Karpel, R. L. (2002). HIV-1 nucleocapsid protein as a nucleic acid chaperone: spectroscopic study of its helix-destabilizing properties, structural binding specificity, and annealing activity. *J. Mol. Biol.* **318**, 749–764.
29. Chan, B., Weidemaier, K., Yip, W. T., Barbara, P. F. & Musier-Forsyth, K. (1999). Intra-tRNA distance measurements for nucleocapsid protein dependent tRNA unwinding during priming of HIV reverse transcription. *Proc. Natl Acad. Sci. USA*, **96**, 459–464.
30. Tisné, C., Roques, B. P. & Dardel, F. (2001). Heteronuclear NMR studies of the interaction of tRNA(Lys)3 with HIV-1 nucleocapsid protein. *J. Mol. Biol.* **306**, 443–454.
31. Hargittai, M. R., Mangla, A. T., Gorelick, R. J. & Musier-Forsyth, K. (2001). HIV-1 nucleocapsid protein zinc finger structures induce $tRNA^{Lys,3}$ structural changes but are not critical for primer/template annealing. *J. Mol. Biol.* **312**, 985–997.
32. Lapadat-Tapolsky, M., Gabus, C., Rau, M. & Darlix, J. L. (1997). Possible roles of HIV-1 nucleocapsid protein in the specificity of proviral DNA synthesis and in its variability. *J. Mol. Biol.* **268**, 250–260.
33. Driscoll, M. D. & Hughes, S. H. (2000). Human immunodeficiency virus type 1 nucleocapsid protein can prevent self-priming of minus-strand strong stop DNA by promoting the annealing of short oligonucleotides to hairpin sequences. *J. Virol.* **74**, 8785–8792.
34. Kim, J. K., Palaniappan, C., Wu, W., Fay, P. J. & Bambara, R. A. (1997). Evidence for a unique mechanism of strand transfer from the transactivation response region of HIV-1. *J. Biol. Chem.* **272**, 16769–16777.

35. Brulé, F., Bec, G., Keith, G., Le Grice, S. F., Roques, B. P., Ehresmann, B. *et al.* (2000). *In vitro* evidence for the interaction of $tRNA_3^{Lys}$ with U3 during the first strand transfer of HIV-1 reverse transcription. *Nucl. Acids Res.* **28**, 634–640.
36. Driscoll, M. D., Golinelli, M. P. & Hughes, S. H. (2001). *In vitro* analysis of human immunodeficiency virus type 1 minus-strand strong-stop DNA synthesis and genomic RNA processing. *J. Virol.* **75**, 672–686.
37. Bernacchi, S., Stoylov, S., Piémont, E., Ficheux, D., Roques, B. P., Darlix, J. L. & Mély, Y. (2002). HIV-1 nucleocapsid protein activates transient melting of least stable parts of the secondary structure of TAR and its complementary sequence. *J. Mol. Biol.* **317**, 385–399.
38. Guo, J., Wu, T., Bess, J., Henderson, L. E. & Levin, J. G. D. (1998). Actinomycin D inhibits human immunodeficiency virus type 1 minus-strand transfer in *in vitro* and endogenous reverse transcriptase assays. *J. Virol.* **72**, 6716–6724.
39. Stryer, L. (1978). Fluorescence energy transfer as a spectroscopic ruler. *Annu. Rev. Biochem.*, **47**, 819–846.
40. Clegg, R. M. (1992). Fluorescence resonance energy transfer and nucleic acids. *Methods Enzymol.* **211**, 353–388.
41. Torimura, M., Kurata, S., Yamada, K., Yokomaku, T., Kamagata, Y., Kanagawa, T. & Kurane, R. (2001). Fluorescence-quenching phenomenon by photoinduced electron transfer between a fluorescent dye and a nucleotide base. *Anal. Sci.* **17**, 155–160.
42. Kurata, S., Kanagawa, T., Yamada, K., Torimura, M., Yokomaku, T., Kamagata, Y. & Kurane, R. (2001). Fluorescent quenching-based quantitative detection of specific DNA/RNA using a BODIPY® FL-labeled probe or primer. *Nucl. Acids Res.* **29**, E34.
43. Wu, W., Henderson, L. E., Copeland, T. D., Gorelick, R. J., Bosche, W. J., Rein, A. & Levin, J. G. (1996). Human immunodeficiency virus type 1 nucleocapsid protein reduces reverse transcriptase pausing at a secondary structure near the murine leukemia virus polypurine tract. *J. Virol.* **70**, 7132–7142.
44. SantaLucia, J. (1998). A unified view of polymer, dumbbell, and oligonucleotide DNA nearest-neighbor thermodynamics. *Proc. Natl Acad. Sci. USA*, **95**, 1460–1465.
45. Lapadat-Tapolsky, M., Pernelle, C., Borie, C. & Darlix, J. L. (1995). Analysis of the nucleic acid annealing activities of nucleocapsid protein from HIV-1. *Nucl. Acids Res.* **23**, 2434–2441.
46. Johnson, P. E., Turner, R. B., Wu, Z. R., Hairston, L., Guo, J., Levin, J. G. & Summers, M. F. (2000). A mechanism for plus-strand transfer enhancement by the HIV-1 nucleocapsid protein during reverse transcription. *Biochemistry*, **39**, 9084–9091.
47. Davanloo, P., Rosenberg, A. H., Dunn, J. J. & Studier, F. W. (1984). Cloning and expression of the gene for bacteriophage T7 RNA polymerase. *Proc. Natl Acad. Sci. USA*, **81**, 2035–2039.
48. Guo, J., Wu, W., Yuan, Z. Y., Post, K., Crouch, R. J. & Levin, J. G. (1995). Defects in primer-template binding, processive DNA synthesis, and RNase H activity associated with chimeric reverse transcriptases having the murine leukemia virus polymerase domain joined to *Escherichia coli* RNase H. *Biochemistry*, **34**, 5018–5029.
49. Birch, D. J. S. & Imhof, R. E. (1991). *Topics in Fluorescence Spectroscopy* (Lakowicz, J. R., ed.), vol. 1, pp. 64–71, Plenum Press, New York.
50. Shen, J. & Snook, R. D. (1989). Thermal lens measurement of absolute quantum yields using quenched fluorescent samples as references. *Chem. Phys. Letters*, **155**, 583–586.
51. Norman, D. G., Grainger, R. J., Uhrin, D. & Lilley, D. M. J. (2000). Location of cyanine-3 on double-stranded DNA: Importance for fluorescence resonance energy transfer studies. *Biochemistry*, **39**, 6317–6324.
52. Förster, T. (1948). Intermolecular energy migration and fluorescence. *Ann. Phys.* **2**, 55–75.

Edited by M. F. Summers

(Received 12 August 2002; received in revised form 14 October 2002; accepted 14 October 2002)